Membrane Current Following Activity in Canine Cardiac Purkinje Fibers

ROBIN T. FALK and IRA S. COHEN

From the Department of Physiology and Biophysics, State University of New York at Stony Brook, Stony Brook, New York 11794

ABSTRACT Membrane current following prolonged periods of rapid stimulation was examined in short (<1.5 mm) canine cardiac Purkinje fibers of radius <0.15 mm. The Purkinje fibers were repetitively stimulated by delivering trains of depolarizing voltage clamp pulses at rapid frequencies. The slowly decaying outward current following repetitive stimulation ("post-drive" current) is eliminated by the addition of 10^{-5} M dihydro-ouabain. The post-drive current is attributed to enhanced Na/K exchange caused by Na loading during the overdrive. Depolarizing voltage clamp pulses initiated from negative (−80 mV) or depolarized (−50 mV) holding potentials can give rise to post-drive current because of activation of tetrodotoxin-sensitive or D600-sensitive channels. The magnitude of the post-drive current depends on the frequency of voltage clamp pulses, the duration of each pulse, and the duration of the repetitive stimulation. The time constant of decay of the post-drive current depends on extracellular [K] in accordance with Michaelis-Menten kinetics. The K_m is 1.2 mM bulk [K], $[K]_B$. The mean time constant in 4 mM $[K]_B$ is 83 s. Epinephrine (10^{-5} M) decreases the time constant by 20%. The time constant is increased by lowering $[Ca]_o$ between 4 and 1 mM. Lowering $[Ca]_o$ further, to 0.1 mM, eliminates post-drive current following repetitive stimulation initiated from depolarized potentials. The latter result suggests that slow inward Ca^{2+} current may increase $[Na]_i$ via Na/Ca exchange.

INTRODUCTION

The automaticity of cardiac tissue is initially suppressed after repetitive stimulation at rates exceeding its normal spontaneous rate. This phenomenon, called "overdrive suppression," was first described one hundred years ago by Gaskell (1884). Activation of electrogenic Na/K exchange resulting from a rise in intracellular sodium concentration during the repetitive stimulation has been proposed to contribute to the membrane potential hyperpolarization and consequent suppression of automaticity (Vassalle, 1970). Cardiac glycosides, which are specific inhibitors of the Na/K pump, affect the magnitude and duration of the post-drive hyperpolarization (Carpentier and Vassalle, 1971).

Address reprint requests to Dr. Ira S. Cohen, Dept. of Physiology and Biophysics, SUNY at Stony Brook, Stony Brook, NY 11794. Dr. Falk's present address is Physiologisches Institut, Universitat Bern, Bern, Switzerland.

J. GEN. PHYSIOL. © The Rockefeller University Press · 0022-1295/84/05/0771/29 $1.00

Volume 83 May 1984 771–799

Although evidence strongly suggests that the post-drive hyperpolarization is due to electrogenic Na/K exchange, the origin of the "sodium load" remains uncertain. It seems likely that the increase in $[Na]_i$ is due at least in part to sodium influx through the tetrodotoxin (TTX)-sensitive fast inward channel. This idea is supported by the reduced effectiveness of overdrive from depolarized potentials in Purkinje fibers (Hoffman and Dangman, 1982).

The present study employs the voltage clamp and canine cardiac Purkinje fibers to study the membrane current that follows a period of rapid activity. We present evidence from application of dihydro-ouabain (DHO) and changes in bathing [K] that identifies post-activity current as Na/K pump current. Further, we find that current flow through either fast inward (TTX-sensitive) or slow inward (D600-sensitive) channels can contribute to the elevation of $[Na]_i$ that gives rise to post-drive current. Finally, we examine the effects of [Ca], temperature, and epinephrine on the decay rate constant of the post-drive current. Preliminary results of this work have appeared in abstract form (Falk and Cohen 1981, 1982, 1983).

METHODS

Adult mongrel dogs were anesthetized with either pentobarbital or a euthanasia solution (T61; American Hoechst Corp., Somerville, NJ). Free-running Purkinje fibers were dissected from both ventricles, leaving small pieces of ventricle (<1 mm in diameter) still attached. These preparations were allowed to recover for 1–2 h. The ventricle was then cut away and Purkinje fibers <0.3 mm in diameter were sectioned into lengths of <1.5 mm. A second recovery period of 1–2 h followed. During recovery, field stimulation was delivered at a frequency of 1 Hz. In more recent experiments, the recovery periods were shortened to the time taken for preparations in each stage of dissection to begin to contract in response to the field stimulation (as short as 15 min).

A two-microelectrode voltage clamp was used (Deck et al., 1964; Cohen et al., 1976, 1983). The voltage clamp (Pedclamp MK6) was designed by Wilf Laycock and Denis Noble, and fabricated in the electronics shop of the University Laboratory of Physiology at Oxford. Conventional intracellular glass microelectrodes, filled with 3 M KCl and having tip resistances between 15 and 25 MΩ, were bevelled to 4–5 MΩ using a thick slurry method (Lederer et al., 1979). Data were recorded on a chart recorder (model 2200S; Gould, Inc., Cleveland, OH). Current records were filtered at a frequency of 5 Hz, unless otherwise noted.

The fibers were repetitively stimulated by applying trains of voltage clamp pulses of brief duration. During approximately the first 10 ms of depolarization the membrane potential "escapes" from voltage clamp control because of activation of the fast inward sodium current. Therefore, the initial onset of depolarization can be considered a modified action potential upstroke, altered by the voltage clamp. After the train of depolarizing voltage clamp pulses, the potential was clamped to the holding potential during the overdrive, unless otherwise noted. The membrane current during the overdrive was usually not recorded since it was more inward than the post-drive current. Recording the current during the overdrive necessitated repositioning of the recorder pen, which moved the holding current level by an unknown amount (the zero-current level was then monitored more often).

Time constants (τ) of post-drive current decay were determined by log-linear regression analysis. In a few cases there were no deviations from a single exponential decay, and a

line was drawn by eye. All the current magnitudes and integrals were determined assuming a single exponential decay. The initial current magnitude was the y-intercept of the best fit to the post-drive current decay. The integral was the product of this initial current magnitude (I_o) with the time constant of decay (τ). In some experiments deviations from a single exponential decay existed during the first 30 s after the termination of activity. For such results the initial 30-s time period was excluded in estimating τ.

The volume of the tissue bath was 2–3 ml and the flow rate was 6–10 ml/min, permitting the bath solution composition to be changed within 3 min. Control solutions contained 140 mM NaCl, 4 mM KCl, 4 mM $CaCl_2$ (unless otherwise noted), 2 mM $MgCl_2$, 12 mM $NaHCO_3$, 0.4 mM NaH_2PO_4, and 1.5 g·liter^{-1} glucose, and were bubbled with 95% O_2/5% CO_2. The fibers were dissected and recovered in 4 mM [Ca]-Tyrode at <33°C (4 mM [Ca]/8 mM [K]-Tyrode in more recent experiments). The pH in the open tissue bath was 7.4 ± 0.1. TTX (Sigma Chemical Co., St. Louis, MO) and D600 (courtesy of Knoll, Federal Republic of Germany) were applied at concentrations of 3×10^{-5} M and 5×10^{-6} g/ml (~10 μM), respectively. DHO (Sigma Chemical Co.) was added to the perfusion solution from a 1-mM stock containing ethanol, such that the final concentration of ethanol was <0.1% by volume. The L-epinephrine (Calbiochem-Behring Corp., San Diego, CA) concentrations are specified in the text.

RESULTS

Post-Drive Membrane Current Induced by Trains of Brief Depolarizing Voltage Clamp Pulses

We previously reported that a slowly decaying outward current occurs following activity in canine Purkinje fibers (Kline et al., 1980; Cohen et al., 1981). In those experiments, field stimulation was applied at rapid frequencies (1–2 Hz) for prolonged periods (0.5–5 min) and after the activity the membrane potential was voltage clamped. As previously described, we standardized the overdrive by applying trains of brief-duration depolarizing voltage clamp pulses delivered at rapid frequencies (Fig. 1). This enabled control of the membrane potential during the overdrive (except during the first 10 ms of depolarization), the duration of depolarization, and the interval between depolarizations. The membrane potential escapes from voltage clamp control during the first 10 ms of depolarization on activation of the large inward TTX-sensitive sodium current.

In Fig. 1*A*, voltage clamp pulses of 50 ms duration, delivered every 100 ms from a holding potential of −73 mV to a pulse potential of −30 mV, were applied for 30 s (top), 1 min (middle), and 2 min (bottom). Following overdrive the membrane potential was clamped at the holding potential. Longer periods of overdrive induce more post-drive current. Post-drive currents shown in Fig. 1*A* are plotted on semilogarithmic coordinates in Fig. 1*B*. The decay of the current is fit by a single exponential (see Discussion). Post-drive current decayed with a time constant of 72 s in this fiber. The time constant is relatively independent of the duration of overdrive. The mean time constant induced by overdrives lasting >1 min (1.5–3 min), normalized to the time constant induced by 1 min of overdrive, is 1.01 ± 0.11 (± SEM, $n = 8$).

Post-Drive Current Induced from a Depolarized Potential

Post-drive current induced from either a depolarized or negative holding poten-

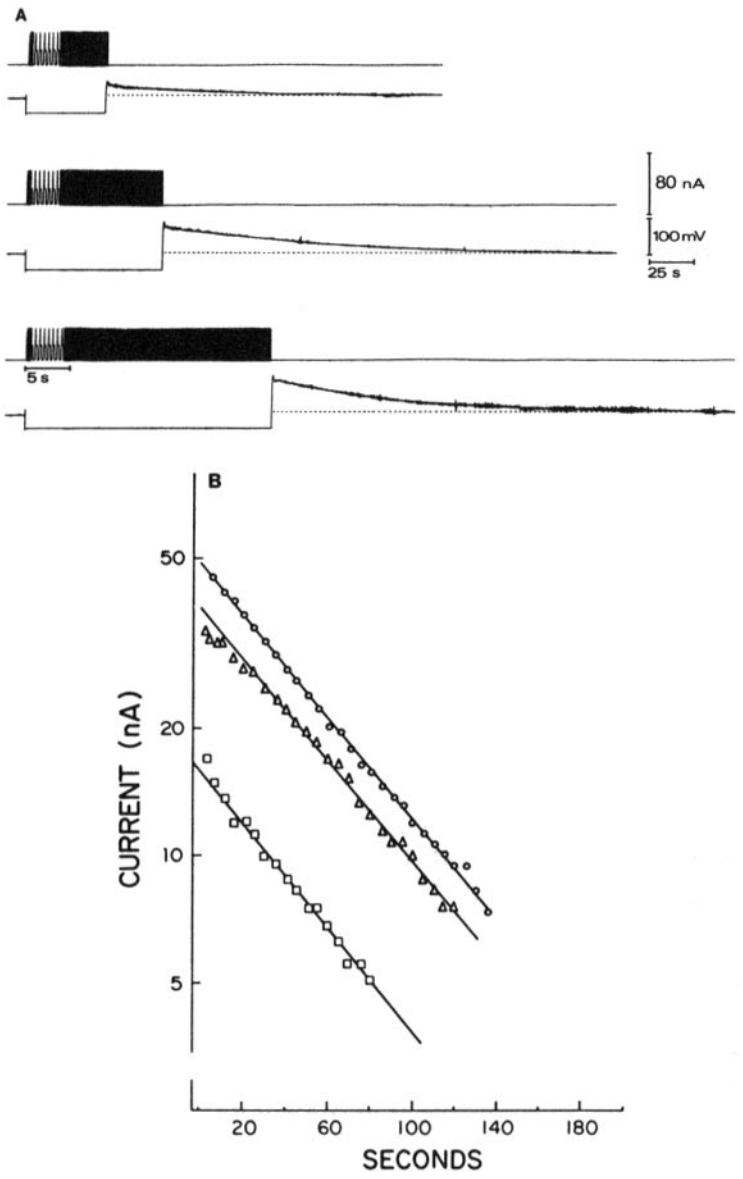

FIGURE 1. Membrane current following trains of brief depolarizing voltage clamp pulses. (*A*) Voltage clamp pulses of 50 ms duration, from a holding potential (V_H) of −73 mV to a pulse potential (V_p) of −30 mV, were delivered at a frequency of 10 Hz for 30 s (top), 1 min (middle), and 2 min (lower). In each pair of records the upper trace is voltage and the lower trace is current. (*B*) Semilogarithmic plot of current traces in *A*. 30 s (□), 1 min (△), and 2 min (○). The membrane potential escapes from the control of the voltage clamp during the first 10 ms (see text and Methods). Following overdrive, the potential was clamped at V_H = −73 mV. The dashed lines indicate the holding current (I_H) following the overdrive. I_H was −20 nA at −73 mV. The horizontal gain was briefly expanded during the drive so that the voltage clamp pulses could be seen. (*B*) Semilogarithmic plots of the currents shown in *A*. The decays can be fit with time constants of 72 s. 34.0 ± 0.1°C. 92480/1. Current records were filtered at 10 Hz.

tial decays with the same time course. An example of this is shown in Fig. 2*A*, in which overdrive was initiated from both −73 (open circles) and −52 mV (solid circles). The post-drive currents were both recorded at −73 mV. The time constant is also independent of the potential at which it is recorded, for potentials negative to −40 mV. In Fig. 2*B*, post-drive current was recorded at the same potential as the holding potential during the overdrive. The mean time constant following overdrive from a depolarized potential (−50 to −54 mV), normalized to that following overdrive from a negative potential (−71 to −78 mV), is 1.03 ± 0.07 (± SEM, $n = 8$).

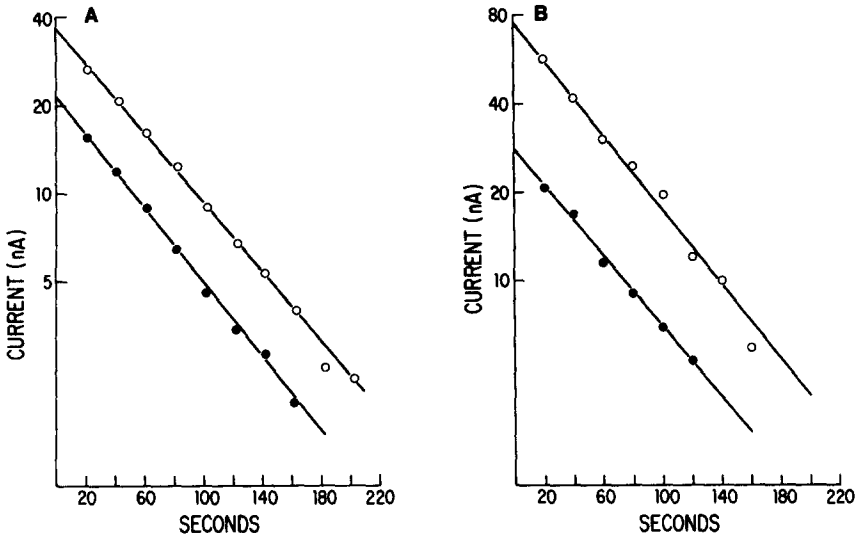

FIGURE 2. The post-drive current time constant is independent of the holding potential. (*A*) Semilogarithmic plots of post-drive current induced from −73 to −30 mV (○) and from −52 to −30 mV (●). Voltage clamp pulses of 50 ms duration were applied at a frequency of 10 Hz for 1 min. The post-drive currents were recorded at −73 mV. The decays can be fit with time constants of 73 (○) and 70 s (●). The maximum diastolic potential (MDP) was −92 mV and I_H was outward relative to zero current at −73 mV. 37 ± 0.1°C. 31081/2. (*B*) Semilogarithmic plots of post-drive current induced from −71 to −13 mV (○) and from −50 to −15 mV (●). Post-drive current was recorded at the same potential as the holding potential during the drive. Voltage clamp pulses of 50 ms duration were delivered at a frequency of 10 Hz for 1 min. The decays can be fit with time constants of 69 (○) and 73 s (●). The resting potential was −70 mV. 34.5 ± 0.1°C. 11481/3.

Effects of TTX and D600 on the Post-Drive Current

Current flow through either TTX-sensitive or D600-sensitive channels during an overdrive can give rise to post-drive current (Fig. 3). Addition of TTX (3×10^{-5} M) eliminates post-drive current induced by voltage clamp pulses from −75 to −37 mV (Fig. 3*A*, left), but has little effect on post-drive current induced by

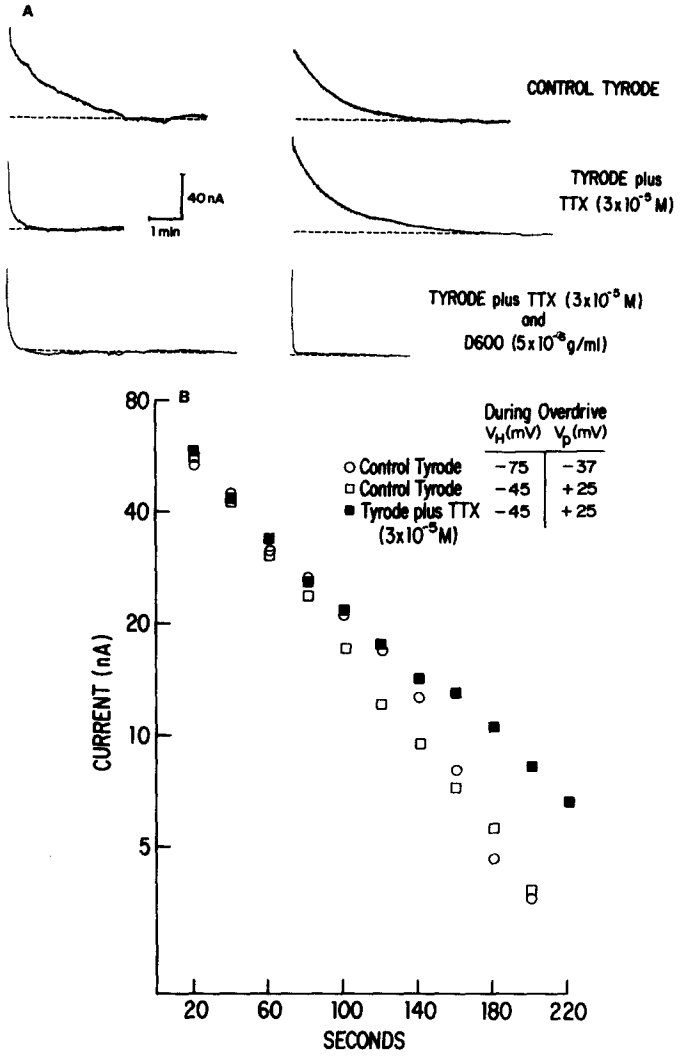

FIGURE 3. Both TTX-sensitive and D600-sensitive current can generate post-drive current. (*A*) Overdrive was delivered from −75 to −37 mV (current records on left) and from −45 to +25 mV (current records on right). Voltage clamp pulses of 50 ms duration were delivered at a frequency of 10 Hz for 1 min. Upper records: control Tyrode; middle records: on addition of 3×10^{-5} M TTX; lower records: on addition of 5×10^{-6} g/ml D600 to the TTX-containing solution. The MDP prior to entering TTX-containing solution was −85 mV. I_H was −20 nA at −75 mV and −5 nA at −45 mV in control solution. On entering TTX, I_H moved outward by 70 nA (at −45 mV), and on entering D600, I_H moved 10 nA more outward (at −45 mV). In the lower current records (left and right), the steady state holding current after the drive was the same as that before the drive. In the middle left record the steady state holding current after the drive remained 4.0 nA more outward than before the drive. 35.4 ± 0.4°C. (*B*) Semilogarithmic plots of the currents shown in *A*. 61282/1.

voltage clamp pulses from −45 to +25 mV (Fig. 3*A*, right, middle trace). If D600 (5×10^{-6} g/ml) is then added to the TTX-containing perfusion solution, post-drive current induced from depolarized potentials is eliminated (Fig. 3*A*, right, bottom trace). Semilogarithmic plots of the currents following overdrive are shown in Fig. 3*B*.

Effects of DHO

Figs. 4 and 5 show the effects of 10^{-5} M DHO on the post-drive current. In Fig. 4 post-drive current was induced by depolarizing voltage clamp pulses applied from a holding potential of −75 mV. Exposure to 10^{-5} M DHO eliminates the post-drive current (middle panel). On return to control Tyrode, the current is again induced (lower panel). Semilogarithmic plots of the current before and after exposure to DHO are shown in Fig. 4*B*. Post-drive current induced from depolarized potentials is also eliminated by 10^{-5} M DHO (Figs. 5*A* and *B*). The holding potential during the overdrive was −50 mV. A partial recovery was obtained on re-exposure to control Tyrode (lower panel). The absence of current following overdrive in DHO suggests that post-drive current is generated either directly or indirectly by enhanced Na/K exchange.

Dependence of the Magnitude of Post-Drive Current on the Pulse Duration during the Overdrive

Figs. 6 and 7 show the effect of decreasing the voltage clamp pulse duration for post-drive current induced from negative and depolarized holding potentials. The post-drive currents plotted in Fig. 6 were induced by voltage clamp pulses of 50 (open circles) and 10 ms (open squares) delivered from a holding potential of −73 mV. Decreasing the pulse duration did not affect the magnitude of post-drive current. A second set of records from the same fiber is also shown (plusses and ×'s). Decreasing the pulse duration does decrease the magnitude of post-drive current induced from depolarized potentials (Figs. 7*A* and *B*). In record *a* of Fig. 7*A*, 50-ms depolarizing pulses were applied from −50 mV. In record *b*, the pulse duration was reduced to 10 ms, substantially decreasing the current magnitude. After *b* the pulse duration was extended to 50 ms and a larger magnitude of current was again generated (record *c*).

Dependence of the Post-Drive Current Magnitude on Voltage Clamp Pulse Frequency and Duration during Overdrive

Figs. 8–10 show the effect of changing the frequency and duration of the voltage clamp pulses during overdrive from −75 to −41 mV (Fig. 8), −50 to −6 mV (Fig. 9), and −75 to −6 mV (Fig. 10).

In Fig. 8*A*, voltage clamp pulses from −75 to −41 mV were delivered at 5, 10, and 20 Hz. The duration of each voltage clamp pulse was decreased at increased frequencies so that the total time depolarized equaled the total time repolarized for all frequencies. For overdrive from −75 to −41 mV, the relationship between post-drive current and frequency is relatively linear over the frequency range examined. The currents are plotted semilogarithmically in Fig. 8*B*.

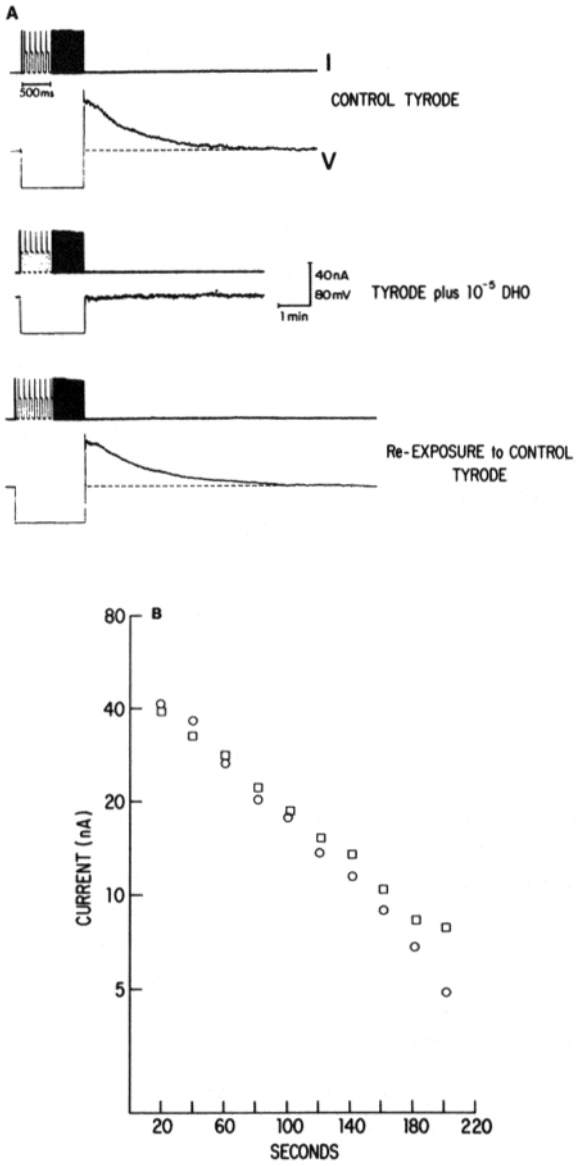

FIGURE 4. Post-drive current induced by overdrive delivered from a holding potential of −75 mV is blocked by DHO. (*A*) The fiber was driven by applying 50-ms voltage clamp pulses, from −75 to −36 mV, at a frequency of 10 Hz for 1 min. Post-drive current, which is present in control Tyrode (upper records), is eliminated on exposure to 10^{-5} M DHO (middle). Overdrive was delivered at 4 min exposure to DHO. The lower records were obtained after return to control Tyrode. The MDP in control Tyrode was −81 mV. I_H was −8.0 nA at −75 mV. On entering DHO, I_H moved inward by 10 nA. 35.0 ± 0.1°C. (*B*) Semilogarithmic plots of post-drive currents shown in *A*. Control Tyrode (○); recontrol (□). 7282/2.

In Fig. 9, voltage clamp pulses from −50 to −6 mV were delivered at frequencies between 2.5 and 20 Hz. The data suggest a nonlinear relationship between post-drive current and frequency. For example, the current induced by overdrive at 10 Hz (Fig. 9*A*, bottom, left) is approximately twice as large as that induced at 2.5 Hz (bottom, right).

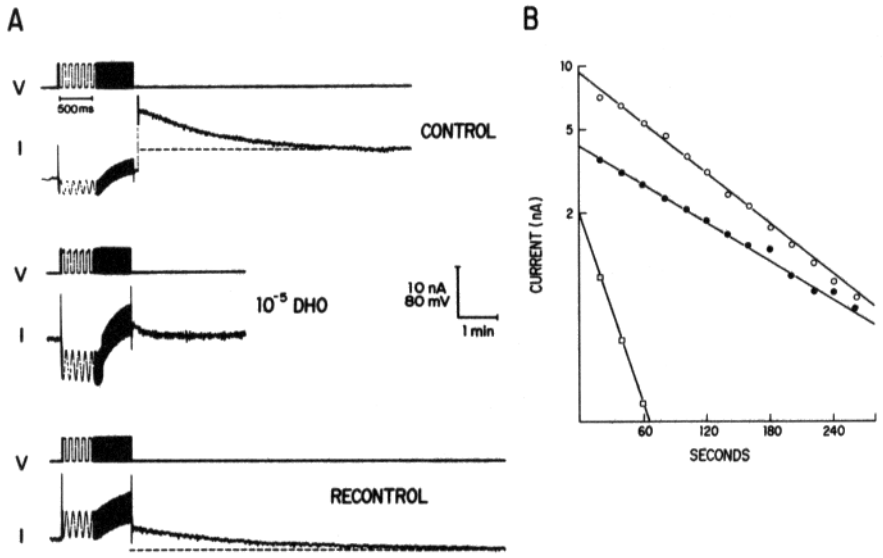

FIGURE 5. Post-drive current induced from a depolarized potential is blocked by DHO. (*A*) Voltage clamp pulses were applied from −50 to −15 mV. Exposure to 10^{-5} M DHO eliminates post-drive current (middle). Overdrive was delivered at 4 min of DHO exposure. The discontinuity in the control current record (upper) at the end of overdrive is due to increasing the gain and repositioning of the pen of the strip chart recorder. I_H was +3.0 nA at −50 mV in control Tyrode. On entering DHO, I_H moved inward by 7.0 nA. 32 ± 0.5°C. (*B*) Semilogarithmic plots of the currents shown in *A*; control (○); DHO (□); recontrol (●). 42882/8.

The currents in Fig. 10 were induced from −75 to −6 mV at frequencies between 5 and 20 Hz. In this case, because the holding potential during the overdrive is negative and the pulse potential extends into the slow inward channel activation range, contributions to Na loading from both TTX-sensitive and slow inward current are expected.

Comparison of the Results with the Predictions of a Simple Model

DEPENDENCE OF THE INTEGRAL OF THE POST-DRIVE CURRENT ON THE FREQUENCY OF VOLTAGE CLAMP PULSES Fig. 11 compares the predictions of a simple model of Na loading through fast or slow inward channels with the results obtained in Figs. 8 (open squares), 9 (open circles), and 10 (open triangles). The model, which is derived in full in the Appendix, depends on four major assumptions: (*a*) both fast and slow inward channels activate instantaneously on depolarization; (*b*) the fast inward channel inactivates completely in <10 ms at 35°C

(Colatsky, 1980); (*c*) the slow inward channel inactivates with a time constant of 155 ms at −6 mV (estimated from Reuter and Scholz, 1977); and (*d*) the Na/K pump rate exhibits a first-order dependence on $[Na]_i$. Assumptions *a–c* are unlikely to be entirely correct. The rates of recovery from inactivation and possible incomplete inactivation for either the fast or slow inward channels are not considered. Furthermore, the experiments cannot elicit a fast inward current without a period of initial escape that must activate the slow inward current to some degree. Nevertheless, within the bounds of qualitative comparison the results and model illustrate a number of important points.

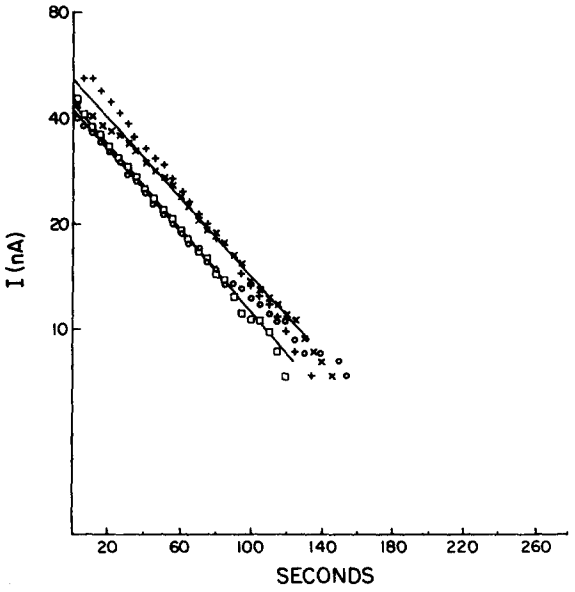

FIGURE 6. Effect of decreasing the pulse duration from 50 to 10 ms on post-drive current induced from a negative potential. Semilogarithmic plots of current after overdrive in which the pulses were 50 (○) and 10 ms (□). The voltage clamp pulses, from −73 to −31 mV, were delivered at 10 Hz for 1.5 min. A second set of records is also shown (50 ms, +; 10 ms, ×). Decreasing the pulse duration did not affect the current. (In some fibers the current magnitude was decreased by a small amount.) The MDP was −89 mV. I_H was −20 nA at −71 mV. 34.8 ± 0.2°C. 92480/1.

The integral of post-drive current, Q, obtained at a given frequency normalized to this integral obtained at the maximum frequency (Q_{max}), is plotted on the ordinate, against frequency on the abscissa in Fig. 11. Q/Q_{max}, obtained by activation of slow inward channels (voltage range −50 to −6 mV), is given as theoretical curve *b* and as the experimentally obtained open circles. Loading through slow inward channels exhibits a less than proportional increase in the ratio Q/Q_{max} when the frequency is raised above 6 Hz. This saturation of the post-drive current integral obtained at high frequencies for sodium loading

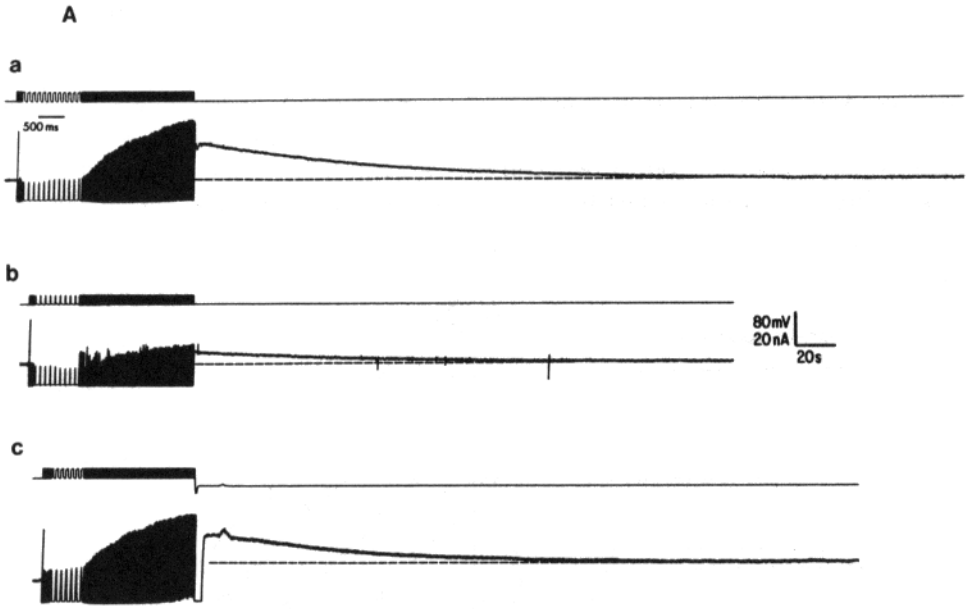

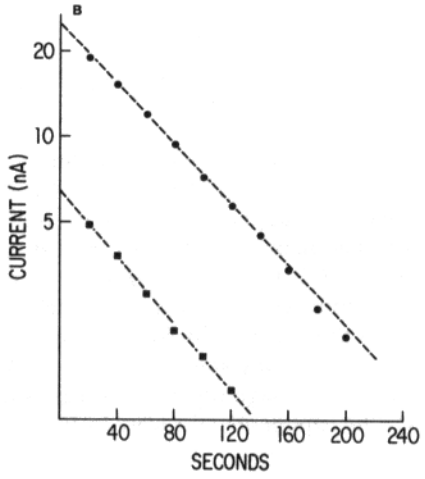

FIGURE 7. Effect of decreasing the pulse duration from 50 to 10 ms on post-drive current induced from a depolarized potential. (*A*) Post-drive currents generated by 50 ms (*a* and *c*) and 10 ms (*b*) voltage clamp pulses. The fiber was driven from −50 to −30 mV at a frequency of 10 Hz for 1 min. (In record *c*, V_H was moved to −73 mV following the overdrive, and the recorder pen was repositioned.) (*B*) Semilogarithmic plots of records *a* (●) and *b* (■). Record *c* is plotted in Fig. 2*A* (■). Figs. 2*A* and 7 are from the same fiber.

through the slow inward channel is in sharp distinction to results obtained with primary activation of the fast inward channel (voltage range −75 to −41 mV), illustrated as the theoretical curve *a* and the experimentally obtained open squares. Activation of both fast and slow inward channels (voltage range −75 to −6 mV), illustrated as theoretical curve *c* and as the experimentally obtained open triangles, yields a result between the two extremes. We constructed curve *c* assuming a 3:1 ratio of fast to slow inward current loading at the maximum

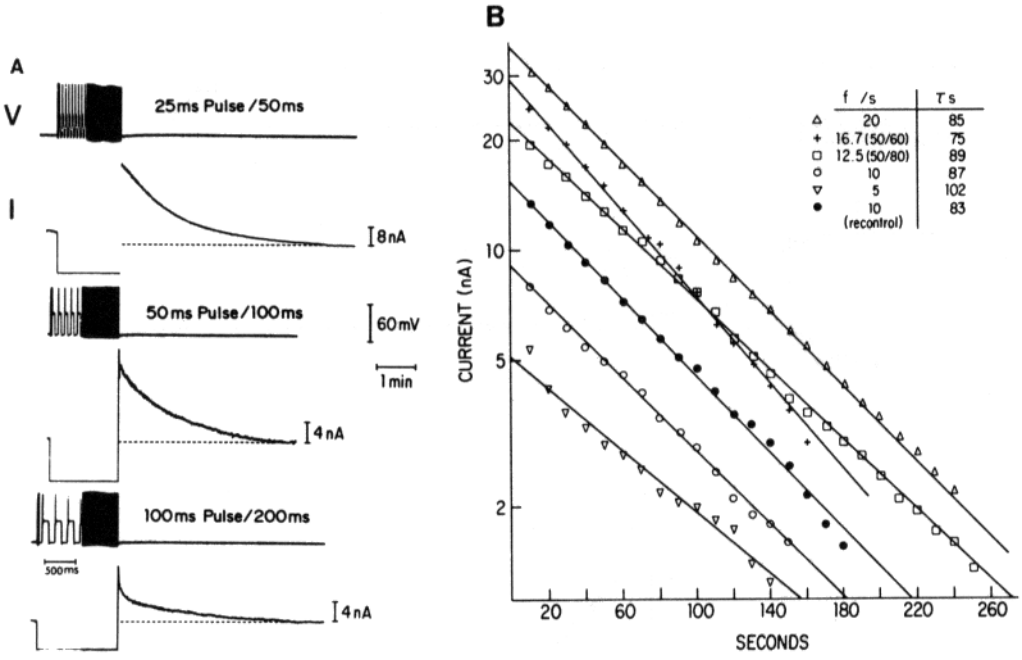

FIGURE 8. Dependence of post-drive current induced from −75 to −41 mV on the frequency and duration of voltage clamp pulses. (*A*) Pulses were delivered at 5, 10, and 20 Hz for 1 min. The upper current record is displayed at half the gain as the two lower records. The maximum diastolic potential was −89 mV and I_H was +6 nA at −75 mV. 36.2 ± 0.2°C. (*B*) Semilogarithmic plots of the currents shown in *A*. Post-drive current induced by 50-ms pulses delivered every 60 ms (+) and every 80 ms (□) are also shown. An additional decay after overdrive at 10 Hz (○) generated less current than the one shown in *A* (●). Both decays were included in the analysis in Fig. 11. Current magnitudes and integrals were determined assuming an exponential decay. The exponential fits were by linear regression analysis (LRA). 102981/1.

frequency because Q_{max} induced by overdrive from −50 to −6 mV was 25% of Q_{max} induced by overdrive from −75 to −6 mV.

DEPENDENCE OF THE INTEGRAL OF POST-DRIVE CURRENT ON OVERDRIVE DURATION Fig. 12 shows the dependence of the integral of post-drive current on the overdrive duration, normalized to that which would be obtained at infinite duration. The data are from nine experiments. The curve is drawn according to

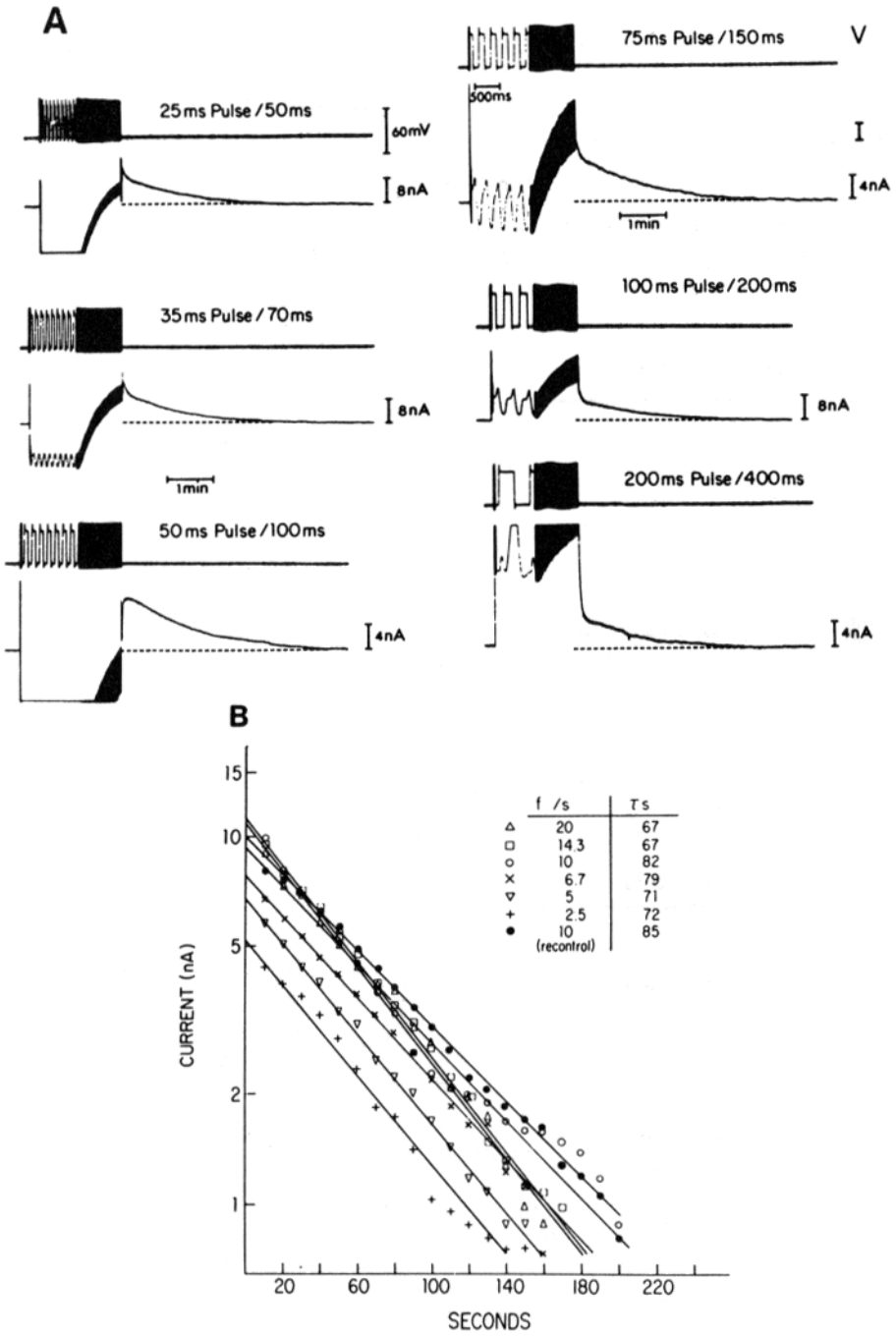

FIGURE 9. Dependence of post-drive current induced from −50 to −6 mV on the frequency and duration of voltage clamp pulses. (*A*) Pulses were delivered at 2.5–20 Hz, as indicated, for 1 min. The current calibration in *A* is 8 nA (left: top and middle; right: middle) and 4 nA (left: bottom; right: top and bottom). The data are from the same fiber as Figs. 8 and 10. The MDP was −95 mV and I_H was +0.8 nA at −50 mV. 36.3 ± 0.25°C. (*B*) Semilogarithmic plots of the currents in *A*. A second decay following overdrive at 10 Hz (●) is also shown. Exponential fits by LRA.

Eq. 2 of the model (see Appendix), which predicts an exponentially saturating relationship between Q/Q_{max} and duration.

Estimated Rise in Intracellular [Na] during the Overdrive

A rough estimate of the rise in $[Na]_i$ during the overdrive can be obtained from the integral of the post-drive current (Q), assuming that Q is linearly proportional

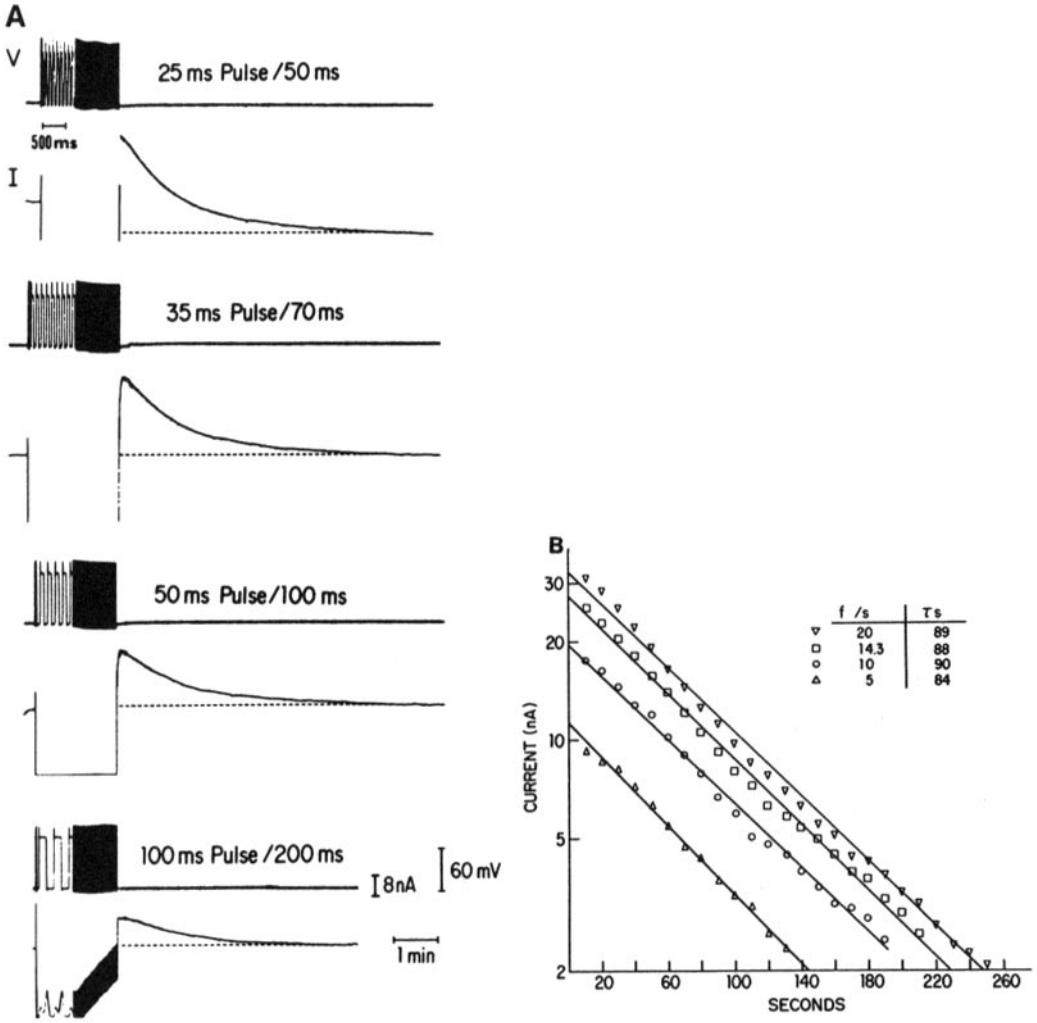

FIGURE 10. Dependence of post-drive current induced from −75 to −6 mV on the frequency and duration of voltage clamp pulses. (*A*) Pulses were delivered at 5–20 Hz for 1 min. (*B*) Semilogarithmic plots of the currents in *A*. I_H was −3.5 nA at −75 mV. 36.3 ± 0.25°C. Exponential fits by LRA. 102981/1.

to $\Delta[Na]_i$. The calculated rise in $[Na]_i$ for drives of 2–4 min ranges between 1 and 5 mM. These calculations assume a Na/K pump coupling ratio of 3:2 and a cellular volume equal to 30% of the estimated fiber volume (Eisenberg and Cohen, 1983).

Having now described the characteristics of the Na loading process, the remainder of the results focus on the properties of the post-drive current.

$[K]_B$ Dependence of the Rate Constant of the Post-Drive Current

The effect of varying the bulk [K], $[K]_B$, between 1 and 8 mM is shown in Fig. 13. The mean normalized rate constants are plotted against $[K]_B$ in Fig. 13*A*. The curve is drawn according to Michaelis-Menten kinetics. On the right (Fig. 13*B*) is a Lineweaver-Burk plot of the same data plotted as the reciprocal of the mean normalized rate constant against the reciprocal of the $[K]_B$. The $[K]_B$ at which the rate constant is half-maximal, the K_m, was obtained from the double reciprocal plot and is 1.2 mM. The mean rate constant in 4 mM $[K]_B$ is 83.2 ± 7.0 s (SEM; the mean rate constant is 0.013 s^{-1}). The maximal rate constant is 0.017 s^{-1}. Table I compares these results with those of Gadsby (1980), in which the rise in internal [Na] results from Na/K pump inhibition caused by exposure to K-free Tyrode. The K_m, maximal rate constants, and mean time constants in 4 mM [K]-Tyrode are in close agreement.

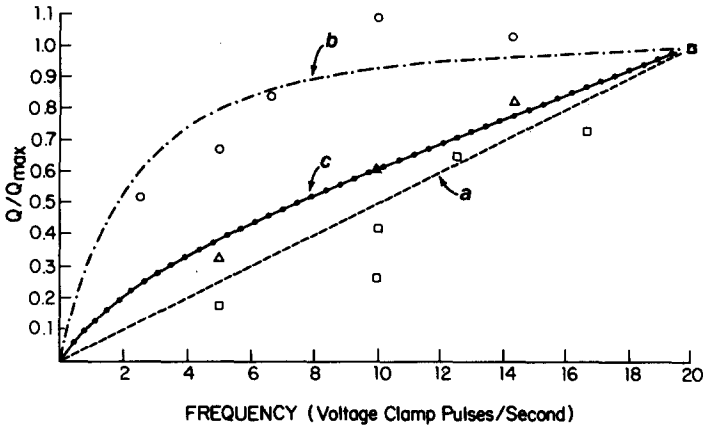

FIGURE 11. Comparison of the data from Figs. 8 (□), 9 (○), and 10 (△) with curves *a–c* of Fig. 17*B* (see text).

Temperature Dependence of the Post-Drive Current

The post-drive currents plotted in Fig. 14*A* were obtained over a temperature range of 28–37°C. The Q_{10} between 28 and 37°C in this fiber was ~3.0, ranging from 2.0 between 33 and 37°C to 4.0 between 28 and 33°C. Fig. 14*B* shows an Arrhenius plot of data from several experiments. The log of the mean rate constant is plotted against the reciprocal of temperature in degrees Kelvin. The points can be fit with a straight line indicating a Q_{10} of 2.5. These findings are in good agreement with the temperature dependence of Na/K pump current following zero-K exposure in sheep Purkinje fibers (Eisner and Lederer, 1980).

Effect of Epinephrine

In Fig. 15, post-drive current in control Tyrode and in the presence of 10^{-5} M epinephrine is plotted on semilogarithmic coordinates. The decays shown in

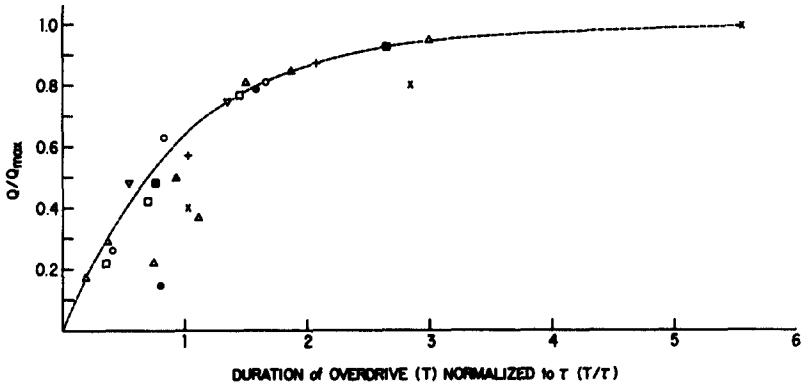

FIGURE 12. Effect of overdrive duration on post-drive current. Q/Q_{max} is plotted against the duration of the overdrive, normalized to the time constant, for nine experiments. The integral of post-drive current (Q) in each experiment was normalized to Q_{max} at infinite duration. Q_{max} for each experiment was calculated by extrapolating the Q obtained at the longest duration examined to infinite duration using Eq. 2. The longest durations examined, then, fall directly on the curve.

Figs. 15*A* and *B* are from the same fiber. Fig. 15*C* shows the results from a second experiment. In each case the time constant is decreased in epinephrine (solid circles) as compared with before (open circles) and after (open squares) epinephrine exposure. Post-drive current was generated by fast and slow inward current during the drive in Fig. 15*A* (i.e., $V_H \doteq -80$ mV; $V_p = -18$ mV) and by slow inward current in Fig. 15*B* (i.e., $V_H = -44$ mV; $V_p = +11$ mV). Epinephrine decreased the time constant by a similar amount in Figs. 15*B* (0.74) and *A* (0.68). The mean normalized time constant in 0.5–1.0 × 10^{-5} M epinephrine from six different fibers is 0.80 ± 0.07 (± SEM).

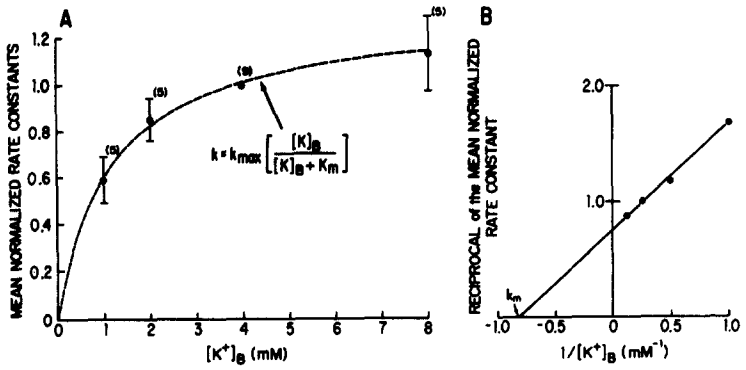

FIGURE 13. The effect of $[K]_B$ on the post-drive current rate constant. (*A*) Mean rate constants, normalized to those in 4 mM $[K]_B$ for each fiber, are plotted against $[K]_B$. The data are from nine experiments. The error bars are ± SEM. The curve is drawn according to the equation indicated. (*B*) A double reciprocal plot of the same data. The straight line was drawn by linear regression analysis (correlation coefficient = 0.9973).

External [Ca] Alters the Magnitude and Time Course of the Post-Drive Current

The effect of varying the external [Ca] between 1 and 8 mM is shown in Table II. The mean normalized time constants, current magnitudes, and integrals of post-drive current are indicated.

The current magnitudes and integrals are decreased in 1, 2, and 2.7 mM [Ca] and increased in 8 mM [Ca]. This may be associated with decreased "escape" of the membrane potential from voltage clamp control (during the first 10 ms of depolarization) in reduced [Ca]. The decrease in escape suggests that less current is flowing through fast inward channels on depolarization, which would decrease $\Delta[Na]_i$ during the drive. The time constants in 1, 2, and 2.7 mM [Ca] are slowed by 10–20%. Averaging the results from all [Ca]'s below 4 mM yields a mean normalized time constant of 1.15 ± 0.04 ($n = 17$).

TABLE I

Comparison of the Effect of $[K^+]_B$ on the Post-Drive Current and on the Current Following Zero-K^+ Exposure

	Zero-K^+ exposure*	Overdrive
K_m (mM)	0.94	1.2
k_{max} (s^{-1})	0.015	0.017
Mean τ (s) in $4[K^+]_B$ (± SEM)	82±4	83±7.0
Temperature (°C)	37±1	35.8
Number of experiments	16	9

Comparison of results from experiments on canine Purkinje fibers in which Na/K pump activity was elevated by prior exposure to K-free Tyrode (left, Gadsby, 1980) and from overdrive (right).

* From Gadsby (1980).

Exposure to 0.1 mM [Ca] Tyrode Virtually Eliminates Post-Drive Current Induced from Depolarized Potentials

Fig. 16 (*A* and *B*) shows the effects of reducing external [Ca] from 2.7 to 0.1 mM in two different fibers (*A* and *B*). In both fibers the holding potential was −45 mV. Post-drive current is present in 2.7 mM [Ca] Tyrode (top records), but in 0.1 mM [Ca] little if any current is induced (middle, bottom records). The drives shown in the two middle records were initiated at 3 and 4 min following exposure to 0.1 mM [Ca]. In the records shown in the lower left, overdrive was initiated from a more negative holding potential (−56 mV). This shift in holding potential suggested the possibility that changes in surface potential had shifted channel gating so that slow inward channels were no longer opening on depolarization.

DISCUSSION

Membrane current through both fast and slow inward channels during overdrive can give rise to post-drive current. Total elimination of the post-drive current by 10^{-5} M DHO indicates that post-drive current is due to enhanced Na/K exchange, which results from the rise in $[Na]_i$ during the period of repetitive stimulation. It is possible that the post-drive current is only indirectly dependent

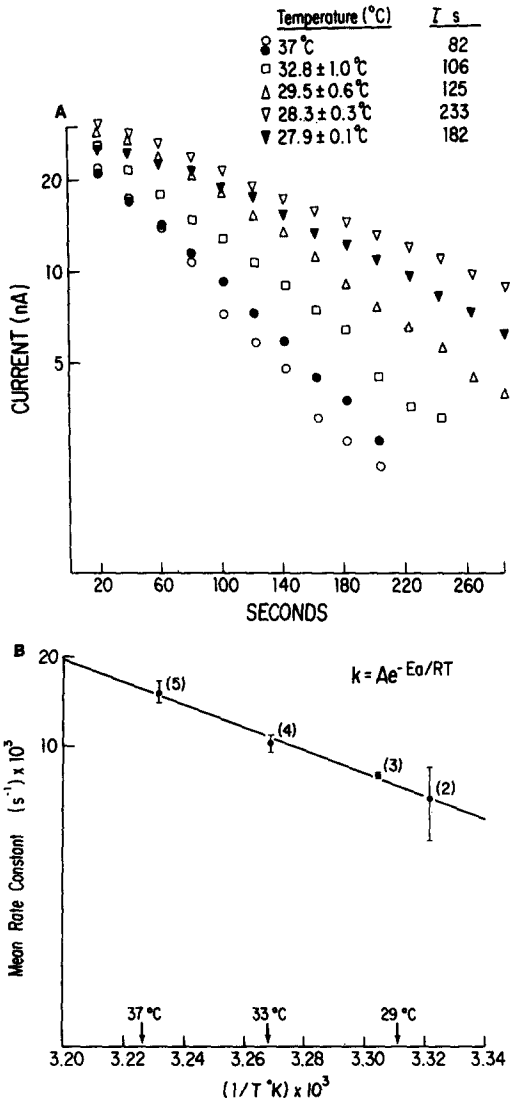

FIGURE 14. The temperature dependence of the post-drive current. (*A*) Semilogarithmic plots of the currents obtained at the indicated temperatures. Voltage clamp pulses were delivered from −66 to −23 mV. The MDP was −81 mV. I_H was +4.5 nA at −66 mV. 2.0 mM [Ca] Tyrode. 81381/2. (*B*) An Arrhenius plot of the temperature dependence of the rate constant. The numbers inside the parentheses refer to the number of experiments. The error bars are ± SEM. Line drawn by LRA (correlation coefficient = −0.9959).

on Na/K pump current, possibly through cleft K depletion. However, the absence of an effect of train length on post-drive current decay time constant and the 1.2-mM K_m for K strongly suggest that post-drive current is Na/K pump current. The effect of TTX and D600 depends on the voltage range over which the

depolarizing pulses are delivered, as expected from the activation and inactivation ranges of each channel. Similarly, the relationship between post-drive current magnitude and the voltage clamp pulse duration and frequency is quite different depending on the voltage range over which the pulses are delivered. These differences, presumably in the relative amounts of Na loading, can be roughly approximated by incorporating the differences in the inactivation rates of the two channels into a first-order kinetic model of Na/K pump activity (see Appendix and Fig. 11).

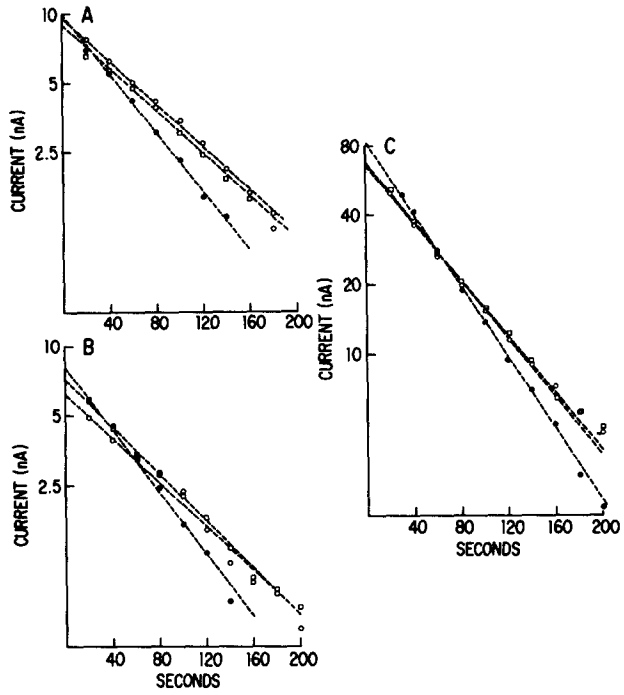

FIGURE 15. The effect of epinephrine on the post-drive current. Semilogarithmic plots of the current in control Tyrode (○, □) and in 10^{-5} M epinephrine (●). Data from two experiments are shown (left: *A* and *B*, right: *C*). The fibers were driven with voltage clamp pulses from −80 to −18 mV (*A*), −44 to +11 mV (*B*), and −75 to −9 mV (*C*). Left (*A* and *B*): 2.7 mM [Ca] Tyrode. I_H moved outward by 7 nA (at −80 mV) on entering epinephrine. 34.8 ± 0.2°C. Same fiber as Fig. 16*B*. 10182/5. (*C*) 2.7 mM [Ca] Tyrode. I_H was −8 nA at −75 mV in control Tyrode and moved inward by 1.2 nA (at −75 mV) on entering epinephrine. 34.6 ± 0.3°C. Same fiber as Fig. 16*A*. 92182/5.

Pumped Na efflux has been observed to show a first-order dependence on $[Na]_i$ in a variety of preparations (Hodgkin and Keynes, 1956; Hodgkin and Horowicz, 1959; Thomas, 1969, 1972; Deitmer and Ellis, 1978; Gadsby and Cranefield, 1979; Eisner and Lederer, 1980; Glitsch and Pusch, 1980). Quantitative descriptions of the decay of Na/K pump activity following Na loading by exposure to K-free solution in sheep and canine Purkinje fibers have been

presented. In these models $[Na]_i$ depends only on pumped Na efflux and passive Na influx, sodium extrusion shows a first-order dependence on $[Na]_i$, and the coupling ratio is independent of both $[Na]_i$ and $[K]_o$ (Eisner and Lederer, 1980; Gadsby, 1980). The independence of post-drive current decay rate and the duration of Na loading is consistent with these results. The recovery rate of a^i_{Na} following repetitive stimulation is also independent of the Na load in sheep Purkinje fibers (C. J. Cohen et al., 1982).

In light of these observations, we compared results from experiments in which pulse frequency and duration (as well as overdrive duration) were varied with the predictions of a simple model (see Appendix for details). The model did not include the effects of slow recovery from inactivation or only partial inactivation of either fast or slow inward channels. Also, the choice of the slow inward channel inactivation time constant (Reuter and Scholz, 1977) is questionable, considering the more rapid inactivation observed in isolated cardiac myocytes (Isenberg and Klockner, 1982). It is therefore not surprising that substantial deviations exist between the model and the experimental results. Besides the inadequacies of the model, certain aspects of the experimental results require further consideration.

TABLE II

Effect of External [Ca] on the Post-Drive Current

$[Ca^{2+}]$	τ	I	Q
mM			
1	1.12±0.05 (4)*	0.51±0.08 (4)*	0.57±0.11 (4)*
2	1.15±0.11 (7)	0.79±0.08 (7)*	0.87±0.06 (7)*
2.7	1.19±0.03 (6)*	0.74±0.04 (5)*	0.87±0.05 (5)*
8	1.00±0.05 (4)	1.29±0.18 (4)	1.30±0.20 (4)

The mean time constants (τ), current magnitudes (I), and integrals of the post-drive current decays (Q) were normalized to those in 4 mM [Ca] for each fiber. ± SEM. The number of experiments is indicated in the parentheses. Data are marked with asterisk if statistically significant (mean ± 2 SEM ≷1). I and Q were calculated assuming that the post-drive current decays exponentially.

For loading through the TTX-sensitive channel, the normalized integral of post-drive current (Q/Q_{max}) at low frequencies of overdrive falls below the predicted linear relationship between Q/Q_{max} and frequency (Fig. 11, curve *a*). The normalized Q at short overdrive durations also falls below the exponentially saturating curve of Q/Q_{max} and overdrive duration (Fig. 12). These deviations may result from underestimating the magnitude of smaller post-drive currents. This would also cause the time constant to be underestimated, causing a larger error in Q.

However, the deviations may be real. If Q is proportional to $\Delta[Na]_i$, then lower frequencies and shorter overdrives may induce smaller elevations in $\Delta[Na]_i$ than predicted. The model implicitly assumes a constant extracellular [K], despite evidence indicating that cleft [K] varies considerably during and following overdrive (e.g., Kline et al., 1980). Variations in cleft [K] during and after the overdrive could account for these deviations. If, after overdrive, cleft [K] becomes depleted for large Na loads, then the deviations may be further increased by systematic errors in measurement. Since Q was calculated assuming

the decay was exponential, larger Na loads may be overestimated. The lag in Q/Q_{max} at low frequencies and short overdrives could be due to a nonproportionality between post-drive current magnitude and $\Delta[Na]_i$. This could arise from the contribution of another current other than the Na/K pump current, which depended on overdrive duration and pulse frequency. The analysis also assumes a constant coupling ratio. The results of several studies suggest that the Na/K pump coupling ratio in Purkinje fibers following exposure to zero-K solution is

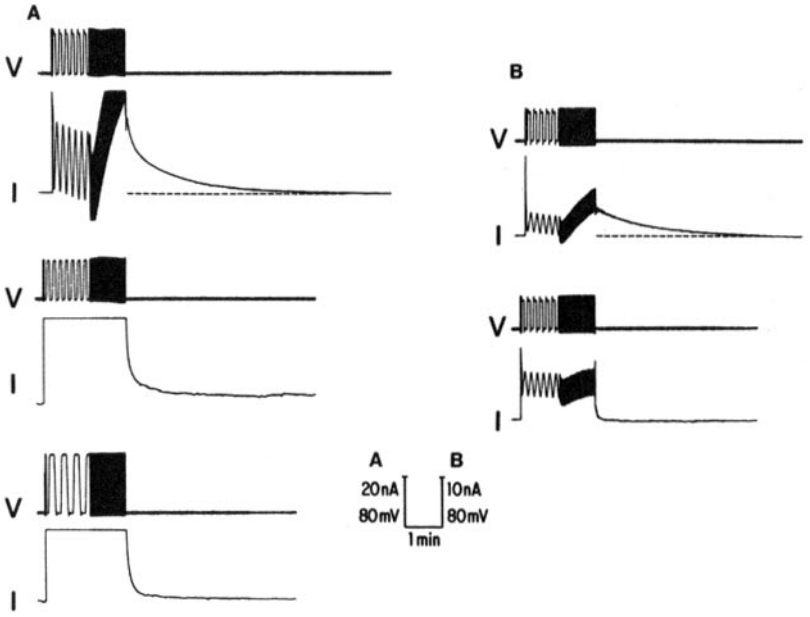

FIGURE 16. Decreasing external [Ca] to 0.1 mM virtually eliminates post-drive current induced from depolarized potentials. 2.7 mM [Ca] control Tyrode (upper records); 0.1 mM [Ca] (middle and lower records). Voltage clamp pulses of 50 ms duration were applied from −45 to +20 mV (*A*: upper and middle) and −45 to +2 mV (*B*: upper and middle) at a frequency of 10 Hz for 1 min. In the lower record of *A* voltage clamp pulses of 100 ms duration were applied from −56 to +40 mV at a frequency of 5 Hz for 1 min. I_H after each of the overdrives in *A* remained more outward than before the drive, but in *B*, I_H returned to its initial value. (*A*) The MDP was −80 mV in control Tyrode. I_H was +8.0 nA at −45 mV. 34.3 ± 0.1°C. 92182/5. (*B*) The MDP was −80 mV in control Tyrode. I_H was −8.5 nA at −45 mV. 34.9 ± 0.1°C. 10182/5.

independent of $\Delta[Na]_i$ (Gadsby, 1980; Eisner et al., 1981; Glitsch and Pusch, 1980). However, an increase in the electrogenicity of the Na/K pump or an uncoupling of Na efflux from K influx with larger $\Delta[Na]_i$ could account for the deviations.

Loading through the Slow Inward Channel during Overdrive Initiated from a Depolarized Potential

We find that repetitive depolarizing pulses delivered from depolarized potentials

generate a post-drive current that is eliminated by either DHO or D600. Post-drive current induced from depolarized potentials is most simply interpreted as Na/K pump current.

It was recently reported that the rise in a^i_{Na} seen during overdrive with voltage clamp pulses applied from −80 to 0 mV is virtually abolished by either depolarizing the potential to −50 mV or by addition of TTX in sheep Purkinje fibers (January et al., 1981; but see our Figs. 3 and 9). It is possible that small changes in a^i_{Na}, of 1 mM, for example, might have been difficult to detect in these experiments. We also previously reported that compared with the amount of post-drive current induced from negative potentials, overdrive from depolarized potentials induced little current (Cohen et al., 1981). However, the contribution of slow inward current to Na loading may be more significant at lower frequencies of overdrive (and longer pulse durations).

The nonlinear relationship between Q/Q_{max} and frequency is roughly accounted for in our model by the slow inactivation rate of the slow inward channel. However, Q/Q_{max} at rapid frequencies decreases as the frequency is further increased (Fig. 11, curve *b*). This could be due to the shortened interval between depolarizing pulses, and may result from incomplete removal of inactivation. Deviations are also suggested by the data at the lowest frequencies. The data suggest that the greatest increase in the Na load per pulse occurs at the longest pulse durations (200 ms), where inactivation rate would have less effect. This may be caused by contributions to loading from slow inward or TTX-sensitive channels remaining open in the steady state (Kass et al., 1976; Reuter and Scholz, 1977; Attwell et al., 1979).

Since most of the slow inward current is carried by Ca and post-drive current disappears in 0.1 mM $[Ca]_o$, it is likely that Na/Ca exchange (Reuter and Seitz, 1968; Glitsch et al., 1970; Baker et al., 1969) contributes to the presumed rise in $[Na]_i$.

Deviations from Exponentiality

We assumed for the purposes of analysis that post-drive current decays exponentially. After the first 30 s the decay can be reasonably well fit by a single exponential. An initial delay, and sometimes an outward current movement, occur prior to the inward decay. The recovery of both a^i_{Na} and membrane potential following repetitive stimulation is also slowed during the first 30–60 s in sheep Purkinje fibers (C. J. Cohen et al., 1982). Depletion of extracellular $[K]_{cleft}$ and/or "contamination" of post-drive current with currents other than the Na/K pump current may contribute to these initial deviations from exponentiality.

Estimates of the Rise in $[Na]_i$ during the Overdrive

The estimated rise in intracellular [Na] during repetitive stimulation at 2.5–10 Hz for 2–4 min ranges between 1 and 5 mM. This is in good agreement with Na-selective microelectrode measurements of Δa^i_{Na} during stimulation in sheep Purkinje fibers of ~2.5 mM Δa^i_{Na} for stimulation at 3 Hz for 3 min (C. J. Cohen et al., 1982), and 3 mM Δa^i_{Na} for 3 min of overdrive with voltage clamp pulses delivered from −80 to 0 mV at a frequency of 4 Hz (January et al., 1981).

Elimination of Post-Drive Current by 10^{-5} M DHO

The absence of post-drive current in 10^{-5} M DHO (Figs. 4 and 5) suggests that 10^{-5} M DHO corresponds to a blocking dose of cardiac glycoside. This is somewhat surprising given the 10 times lower potency of DHO as compared with other cardiac glycosides reported in sheep Purkinje fibers and guinea pig ventricle (Deitmer and Ellis, 1978; Daut and Rudel, 1982). We considered the possibility that a large accumulation of intracellular Na might keep a residual fraction of pump sites working at the maximum rate following the drive. However, the holding current quickly returns to its level prior to the drive, so this seems unlikely.

DHO also eliminates post-drive current generated from depolarized potentials (Fig. 5). This is consistent with block of overdrive suppression by cardiac glycosides in canine Purkinje fibers with depolarized maximum diastolic potentials (−55 mV) (Hoffman and Dangman, 1982).

The absence of current following overdrive in DHO makes it unlikely that either Ca-activated K current (Isenberg, 1977) or electrogenic Na/Ca exchange (Horackova and Vassort, 1979; Coraboeuf et al., 1981) substantially contributes to the post-drive current. This finding is particularly striking since both of these currents are expected to be increased under these conditions.

[K] Dependence of the Time Course of the Post-Drive Current

The K_m, the time constant in 4 mM [K] Tyrode, and the maximal rate constant closely agree with those of the Na/K pump current following zero-K exposure in canine Purkinje fibers (Gadsby, 1980; see our Table I). The K_m for K activation of the red blood cell Na/K ATPase is also between 0.9 and 2.1 mM $[K]_o$ (Schwartz et al., 1975). Our K_m of 1.2 mM agrees well with results from zero-K exposure experiments in guinea pig atria, sheep Purkinje fibers, and rabbit Purkinje fibers (Glitsch et al., 1978, 1981; Verdonck, 1982).

Effect of Epinephrine

The increased rate constant in epinephrine (Fig. 15) is consistent with previous studies which suggested that catecholamines increase Na/K pump activity in cardiac tissue (Otsuka, 1958; Vassalle and Barnabei, 1971; Glitsch et al., 1965; Hougen et al., 1981; Wasserstrom et al., 1982), in skeletal muscle (Clausen and Flatman, 1977), and in the isolated Na/K ATPase (Cheng et al., 1977).

Catecholamines, in addition to directly stimulating the Na/K pump, have also been suggested to increase potassium conductance (Gadsby and Cranefield, 1981). Increased Ca influx in epinephrine (Reuter, 1967) could increase outward K current (Isenberg, 1977), thereby raising cleft [K]. However, cleft [K] accumulations of <1.0 mM (above 4 mM) would only increase the rate constant by <5%, at a K_m of 1.2 mM. The effect of catecholamines on the rate constant has been reported to be present at 13.5 mM [K] Tyrode (Coetzee and Carmeliet, 1982), which suggests that catecholamines are not only increasing cleft [K] since they would have little effect at a $[K]_B$ of 13.5 mM.

Effects of 0.1 mM $[Ca]_o$

The absence of post-drive current in 0.1 mM [Ca] Tyrode (Fig. 16) is probably

due to a large reduction in slow inward current. The peak slow inward current would be substantially reduced in 0.1 mM external [Ca] (e.g., Reuter and Scholz, 1977; Marban and Tsien, 1982). Thus, the Na^+ load in 0.1 mM $[Ca]_o$ may be too small to generate a detectable post-drive current, particularly if the decrease in the post-drive current decay rate constant observed between 4 and 1 mM [Ca] was potentiated in 0.1 mM [Ca]. The dramatic decrease in post-drive current in 0.1 mM [Ca] suggests that slow inward Ca current does play a major role in generating post-drive current, presumably through Na/Ca exchange. Unless the slow inward channel conductance to Na is altered in 0.1 mM [Ca], the magnitude of slow inward Na current should remain large. The apparent absence of post-drive current, despite this residual Na current, may be due to our limited ability to detect small slow currents as outlined above.

A shift in channel gating in 0.1 mM [Ca] was examined by initiating the overdrive from a more negative potential. Shifting the holding potential by 10 mV had no effect. This is not too surprising since the bulk divalent cations were reduced by a factor of only 2.3 and since experimental evidence indicates that inward channel activation and inactivation ranges are not shifted in low $[Ca]_o$ (Reuter and Scholz, 1977).

APPENDIX

A Quantitative Description of the Sodium Loading Process and Its Effect on Na/K Pump Activity

The model to be developed is similar to previous descriptions of the sodium removal process following a period in which intracellular [Na] rises because of inhibition of the Na/K pump (Gadsby, 1980; Eisner and Lederer, 1980). These were modified by including an additional term that describes the frequency dependence and channel dependence of the rise in $[Na]_i$ during the overdrive.

The model is based on Eq. 1, which expresses the change in intracellular [Na] and the associated increment in Na/K pump activity resulting from a train of depolarizing voltage clamp pulses delivered at rapid frequencies:

$$\frac{3\Delta[I_p(t)]}{FV} + fL = \frac{d\Delta[Na]_i}{dt} = fL - k\Delta[Na]_i, \tag{1}$$

where $\Delta[I_p(t)]$ is the increment in Na/K pump activity above baseline level; $\Delta[Na]_i$ is the rise in intracellular [Na] above the resting level; k is the rate constant of the post-drive current; L is the rise in intracellular [Na] per depolarizing pulse; and f is the frequency of voltage clamp pulses during the overdrive. The pulse duration depends on the frequency and is equal to $\frac{1}{2}f$. In Eq. 1, F is the Faraday constant and V is the intracellular volume of the preparation. A constant 3:2 coupling ratio for the Na/K pump is assumed.

Eq. 1 assumes that the removal of intracellular Na obeys first-order kinetics (Gadsby, 1980; Eisner and Lederer, 1980) and that the increment in pump activity depends only on the increment in $[Na]_i$.

Integrating Eq. 1:

$$Q = \frac{FVfL(1 - e^{-kt})}{3k}, \tag{2}$$

where Q is one-third of the total additional charge remaining intracellularly at the end of

the drive, expressed as a function of the frequency, the Na load, and the rate constant of the Na/K pump. We obtained experimental estimates of this Q by integrating the post-drive current, assuming that it is entirely Na/K pump current (see Discussion).

Dependence of the Integral of Post-Drive Current on the Frequency of Voltage Clamp Pulses

If L, the rise in $[Na]_i$ per pulse, is independent of frequency, then Q, normalized to Q at the maximum frequency examined, as a function of frequency, is, from Eq. 2:

$$\frac{Q}{Q_{max}} = \frac{f}{f_{max}}. \tag{3}$$

Therefore, if L is constant, the model predicts a linear relationship between Q/Q_{max} and frequency.

Fig. 17*A* schematically illustrates why L might be independent of frequency for loading through the TTX-sensitive fast inward channel, and dependent on frequency for loading through the slow inward channel. The inactivation rate of the TTX-sensitive channel is fast relative to the pulse duration at all frequencies examined (Colatsky, 1980; Gettes and Reuter, 1974). Therefore, the inactivation variable would have reached its steady state value (near zero) by the end of the shortest depolarizing pulse. However, if the slow inward channel inactivation rate is slow (Reuter and Scholz, 1977; see our Discussion) relative to the shortest pulse durations, then increasing the pulse duration would increase the slow inward current per pulse, thereby increasing L.

As noted above, the results in Fig. 9 suggest a nonlinear relationship between post-drive current and the frequency of voltage clamp pulses during the drive. The model was modified to take this nonlinearity into account by considering slow inward channel inactivation. We assumed, for the purposes of the model, that the slow inward channel activates instantaneously and inactivates exponentially. The integral of the slow inward current during each depolarizing pulse is then:

$$\int_0^{1/2f} I_o(e^{-t'/\tau})\, dt', \tag{4}$$

where I_o is the slow inward current at $t' = 0$ (i.e., peak slow inward current, assuming instantaneous activation); t' is the duration of each pulse; f is the frequency of voltage clamp pulses; and $t' = 1/2f$. τ is the inactivation time constant of the slow inward channel at the pulse potential during the overdrive.

From Eqs. 2 and 4:

$$Q = \frac{Vf}{3k}[I_o\tau(1 - e^{-1/2f\tau}) + FL_{Na}](1 - e^{-kt}), \tag{5}$$

where L_{Na} is the Na load due to TTX-sensitive current per depolarizing pulse and F is the Faraday constant. The Na load per depolarizing pulse caused by slow inward current (L_{SI}) is $[I_o\tau(1 - e^{-1/2f\tau})]$. Normalizing Q with respect to Q at the maximum frequency, it can be shown from Eq. 5 that

$$\frac{Q}{Q_{max}} = \frac{f(1 - e^{-1/2f\tau})}{f_{max}(1 - e^{-1/2f\tau_{max}})}(1 - X) + \frac{f}{f_{max}}(X), \tag{6}$$

where X is the fraction of the rise in $[Na]_i$ caused by TTX-sensitive current at the maximum frequency and $(1 - X)$ is the fraction of the rise in $[Na]_i$ caused by slow inward current at the maximum frequency.

The predictions of the model are shown in Fig. 17*B* for a constant L (curve *a*) and for L as a function of frequency (curves *b–e*). Curves *b–d* were generated using an estimated inactivation time constant for the slow inward channel of 155 ms at −6 mV (Reuter and Scholz, 1977). A pulse potential of −6 mV was chosen to correspond to the data in Figs.

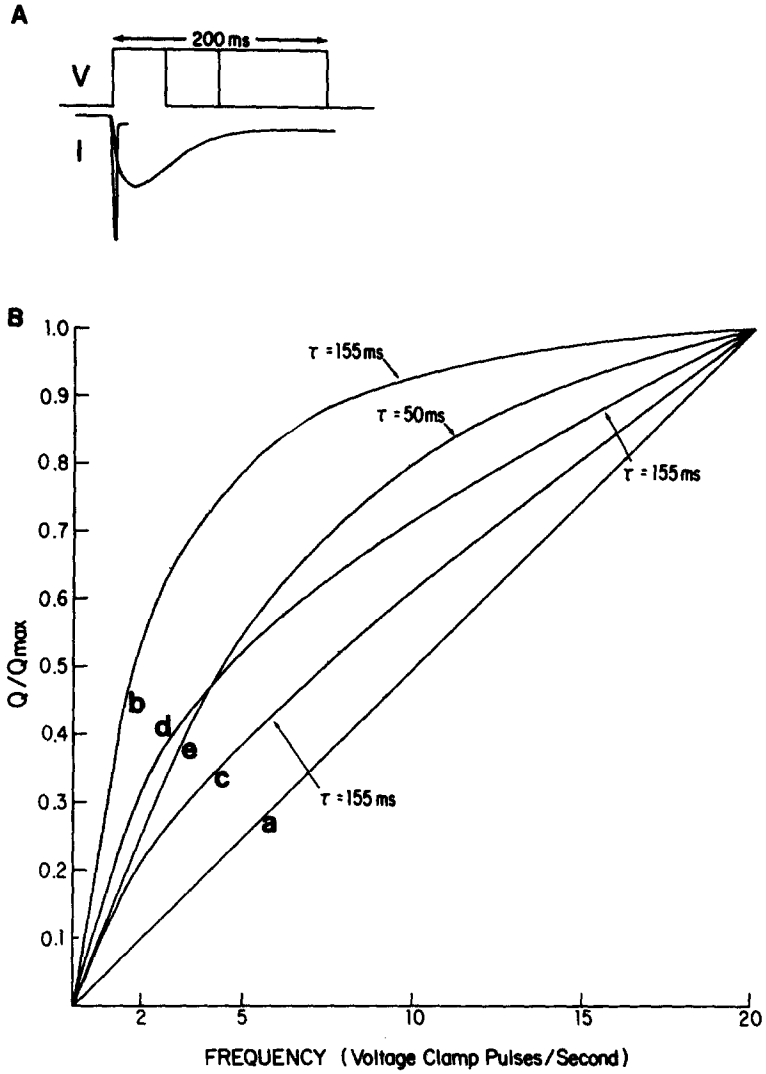

FIGURE 17. Predicted effect of the availability of the fast and slow inward channels on the frequency dependence of post-drive current. (*A*) See text. (*B*) Relationship between Q/Q_{max} and frequency generated by Eq. 6 for all loading through the TTX-sensitive fast channel (*a*); all loading through the slow inward channel, inactivation time constant (τ) = 155 (*b*) and 50 ms (*e*); for 75% TTX-sensitive, 25% slow inward at 20 Hz. τ = 155 ms (*c*); and for 50% TTX-sensitive, 50% slow inward loading at 20 Hz, τ = 155 ms (*d*).

9 and 10. The nonlinearity of the relationship between Q/Q_{max} and frequency becomes less pronounced if some of the rise in $[Na]_i$ is due to current through the TTX-sensitive channel (curves *c* and *d*) or if the slow inward channel inactivates more rapidly (curve *e*).

We would like to thank Dr. Nicholas Datyner, Dr. David Gadsby, Dr. Gary Gintant, Nancy Mulrine, and both journal referees for helpful criticism. This work was performed in partial fulfillment of the Ph.D. degree in Physiology and Biophysics at Stony Brook.
This work was supported by grant HL20558 from the National Heart, Lung and Blood Institute and a grant from the American Heart Association.

Received for publication 3 June 1983 and in revised form 28 December 1983.

REFERENCES

Attwell, D., I. Cohen, D. Eisner, M. Ohba, and C. Ojeda. 1979. The steady state TTX-sensitive ("window") sodium current in cardiac Purkinje fibres. *Pflügers Arch. Eur. J. Physiol.* 379:137–142.

Baker, P. F., M. P. Blaustein, A. L. Hodgkin, and R. A. Steinhardt. 1969. The influence of calcium on sodium efflux in squid axons. *J. Physiol. (Lond.).* 200:431–458.

Carpentier, R., and M. Vassalle. 1971. Enhancement and inhibition of a frequency-activated electrogenic sodium pump in cardiac Purkinje fibers. *In* Research in Physiology, A Liber Memorialis in Honor of Prof. C. McC. Brooks. F. F. Kao, K. Koizumi, and M. Vassalle, editors. Gaggi, Bologna. 81–98.

Cheng, L. C., E. M. Rogus, and K. Zierler. 1977. Catechol, a structural requirement for $(Na^+ + K^+)$-ATPase stimulation in rat skeletal muscle membrane. *Biochim. Biophys. Acta.* 464:338–346.

Clausen, T., and J. A. Flatman. 1977. The effect of catecholamines on Na-K transport and membrane potential in rat soleus muscle. *J. Physiol. (Lond.).* 270:383–414.

Coetzee, A., and E. Carmeliet. 1982. Catecholamines and electrogenic Na Pump in rabbit cardiac Purkinje fibers. *J. Gen. Physiol.* 80:14*a*. (Abstr.)

Cohen, C. J., H. A. Fozzard, and S.-S. Sheu. 1982. Increase in intracellular sodium ion activity during stimulation in mammalian cardiac muscle. *Circ. Res.* 50:651–661.

Cohen, I., J. Daut, and D. Noble. 1976. The effects of potassium and temperature on the pacemaker current, I_{K2}, in Purkinje fibres. *J. Physiol. (Lond.).* 260:55–74.

Cohen, I., R. Falk, and R. P. Kline. 1981. Membrane currents following activity in canine cardiac Purkinje fibers. *Biophys. J.* 33:281–288.

Cohen, I., R. Falk, and R. P. Kline, 1983. Voltage-clamp studies on the canine Purkinje strand. *Proc. R. Soc. Lond. B Biol. Sci.* 217:215–236.

Colatsky, T. 1980. Voltage clamp measurements of sodium channel properties in rabbit cardiac Purkinje fibres. *J. Physiol. (Lond.).* 305:215–234.

Coraboeuf, E., P. Gautier, and P. Guirandou. 1981. Potential and tension changes induced by sodium removal in dog Purkinje fibres: role of an electrogenic sodium-calcium exchange. *J. Physiol. (Lond.).* 311:605–622.

Daut, J., and R. Rudel. 1982. The electrogenic sodium pump in guinea-pig ventricular muscle: inhibition of pump current by cardiac glycosides. *J. Physiol. (Lond.).* 330:243–264.

Deck, K. A., R. Kern, and W. Trautwein. 1964. Voltage clamp technique in mammalian cardiac fibres. *Pflügers Arch. Eur. J. Physiol.* 280:50–62.

Deitmer, J. W., and D. Ellis. 1978. The intracellular sodium activity of cardiac Purkinje fibres during inhibition and reactivation of the Na-K pump. *J. Physiol. (Lond.).* 284:241–259.

Eisenberg, B. R., and I. Cohen. 1983. The ultrastructure of the cardiac Purkinje strand in the dog: a morphometric analysis. *Proc. R. Soc. Lond. B Biol. Sci.* 217:191–213.

Eisner, D. A., and W. J. Lederer. 1980. Characterization of the electrogenic sodium pump in cardiac Purkinje fibres. *J. Physiol. (Lond.).* 303:441–474.

Eisner, D. A., W. J. Lederer, and R. D. Vaughan-Jones. 1981. The dependence of sodium pumping and tension on intracellular sodium activity in voltage-clamped sheep Purkinje fibres. *J. Physiol. (Lond.).* 317:163–187.

Falk, R., and I. Cohen. 1981. Post-drive membrane currents in canine cardiac Purkinje fibers. *Biophys. J.* 33:36*a*. (Abstr.)

Falk, R., and I. Cohen. 1982. Post-drive membrane currents in canine cardiac Purkinje fibers. *Biophys. J.* 37:244*a*. (Abstr.)

Falk, R., and I. Cohen. 1983. Ionic and pharmacological dependence of post-drive current in canine Purkinje fibers. *Biophys. J.* 41:73*a*. (Abstr.)

Gadsby, D. C. 1980. Activation of electrogenic Na^+/K^+ exchange by extracellular K^+ in canine cardiac Purkinje fibres. *Proc. Natl. Acad. Sci. USA.* 77:4035–4039.

Gadsby, D. C., and P. F. Cranefield. 1979. Electrogenic sodium extrusion in cardiac Purkinje fibers. *J. Gen. Physiol.* 73:819–837.

Gadsby, D. C., and P. F. Cranefield. 1981. Isoproterenol hyperpolarization of canine cardiac Purkinje fibers is not mediated by enhanced Na^+/K^+ pump activity. *Biophys. J.* 33:10*a*. (Abstr.)

Gaskell, W. H. 1884. On the innervation of the heart, with especial reference to the heart of the tortoise. *J. Physiol. (Lond.).* 4:43–127.

Gettes, I. S., and H. Reuter. 1974. Slow recovery from inactivation of inward currents in mammalian myocardial fibres. *J. Physiol. (Lond.).* 240:703–724.

Glitsch, H. G., W. Grabowski, and J. Thielen. 1978. Activation of the electrogenic sodium pump in guinea-pig atria by external potassium ions. *J. Physiol. (Lond.)* 276:515–524.

Glitsch, H. G., H. G. Haas, and W. Trautwein. 1965. The effect of adrenaline on the K and Na fluxes in frog atrium. *Naunyn-Schmiedebergs Arch. Exp. Pathol. Pharmakol.* 250:59–71.

Glitsch, H. G., W. Kampmann, and H. Pusch. 1981. Activation of active Na transport in sheep Purkinje fibres by external K and Rb ions. *Pflügers Arch. Eur. J. Physiol.* 391:28–34.

Glitsch, H. G., and H. Pusch. 1980. Correlation between changes in membrane potential and intracellular sodium activity during K activated response in sheep Purkinje fibres. *Pflügers Arch. Eur. J. Physiol.* 384:189–191.

Glitsch, H. G., H. Reuter, and H. Scholz. 1970. The effects of the internal sodium concentration on calcium fluxes in isolated guinea-pig auricles. *J. Physiol. (Lond.).* 209:25–43.

Hodgkin, A. L., and P. Horowicz. 1959. Movements of Na and K in single muscle fibres. *J. Physiol. (Lond.).* 145:405–432.

Hodgkin, A. L., and R. D. Keynes. 1956. Experiments on the injection of substances into squid giant axons by means of a microsyringe. *J. Physiol. (Lond.).* 131:592–616.

Hoffman, B. F., and K. H. Dangman. 1982. Are arrhythmias caused by automatic impulse generation? *In* Normal and Abnormal Conduction in the Heart. A. Paes de Carvalho, B. F. Hoffman, and M. Lieberman, editors. 429–448.

Horackova, M., and G. Vassort. 1979. Sodium-calcium exchange in regulation of cardiac contractility. Evidence for an electrogenic, voltage-dependent mechanism. *J. Gen. Physiol.* 73:403–424.

Hougen, T. J., N. Spicer, and T. W. Smith. 1981. Stimulation of monovalent cation transport by low concentrations of cardiac glycosides. Role of catecholamines. *J. Clin Invest.* 68:1207–1214.

Isenberg, G. 1977. Cardiac Purkinje fibers. $[Ca^{+2}]_i$ controls the potassium permeability via the conductance components g_{k1} and $\bar{g}_{k2}$. *Pflügers Arch. Eur. J. Physiol.* 371:77–85.

Isenberg, G., and U. Klockner. 1982. Calcium currents of isolated bovine ventricular myocytes are fast and of large amplitude. *Pflügers Arch. Eur. J. Physiol.* 395:30–41.

January, C. T., T. E. Bump, and H. A. Fozzard. 1981. Effects of membrane potential on the intracellular sodium activity of Purkinje and ventricular muscle. *Circulation.* 64(Suppl. IV):49. (Abstr.)

Kass, R. S., S. Siegelbaum, and R. W. Tsien. 1976. Incomplete inactivation of the slow inward current in cardiac Purkinje fibres. *J. Physiol. (Lond.).* 263:127–128p.

Kline, R. P., I. Cohen, R. Falk, and J. Kupersmith. 1980. Activity-dependent extracellular K^+ fluctuations in canine Purkinje fibres. *Nature (Lond.).* 286:68–71.

Lederer, W. J., A. J. Spindler, and D. A. Eisner. 1979. Thick slurry bevelling: a new technique for bevelling extremely fine microelectrodes and micropipettes. *Pflügers Arch. Eur. J. Physiol.* 381:287–288.

Marban, E., and R. W. Tsien. 1982. Effects of nystatin-mediated intracellular ion substitution on membrane currents in calf Purkinje fibres. *J. Physiol. (Lond.).* 329:569–587.

Otsuka, M. 1958. Die Wirkung von Adrenalin auf Purkinje-Fasern von Saugetiierherzen. *Pflügers Arch. Eur. J. Physiol.* 266:512–517.

Reuter, H. 1967. The dependence of slow inward current in Purkinje fibers on the extracellular calcium concentration. *J. Physiol. (Lond.).* 192:479–492.

Reuter, H., and H. Scholz. 1977. A study of the ion selectivity and the kinetic properties of the calcium-dependent slow inward current in mammalian cardiac muscle. *J. Physiol. (Lond.).* 264:17–47.

Reuter, H., and N. Seitz. 1968. The dependence of calcium efflux from cardiac muscle on temperature and external ion composition. *J. Physiol. (Lond.).* 195:451–470.

Schwartz, A., G. E. Lindenmayer, and J. C. Allen. 1975. The sodium-potassium adenosine triphosphatase: pharmacological, physiological and biochemical aspects. *Pharmacol. Rev.* 27(1):3–134.

Thomas, R. 1969. Membrane current and intracellular sodium changes in a snail neurone during extrusion of injected sodium. *J. Physiol. (Lond.).* 201:495–514.

Thomas, R. 1972. Intracellular sodium activity and the sodium pump in snail neurons. *J. Physiol. (Lond.).* 220:55–71.

Vassalle, M. 1970. Electrogenic suppression of automaticity in sheep and dog Purkinje fibers. *Circ. Res.* 27:361–377.

Vassalle, M., and O. Barnabei. 1971. Norepinephrine and potassium fluxes in cardiac Purkinje fibers. *Pflügers Arch. Eur. J. Physiol.* 322:287–303.

Verdonck, F. 1982. Activation of sodium pump current in rabbit Purkinje fibers. *J. Gen. Physiol.* 80:24*a*. (Abstr.)

Wasserstrom, J. A., D. J. Schwartz, and H. A. Fozzard. 1982. Catecholamine effects on intracellular sodium activity and tension in dog heart. *Am. J. Physiol.* 243:H670–H675.